Contribution from the Department of Chemistry,
The University of Calgary, Calgary, Alberta, T2N 1N4 Canada

Theoretical Study on the Stability of $M(PH_3)_2(O_2)$, $M(PH_3)_2(C_2H_2)$, and $M(PH_3)_2(C_2H_4)$ (M = Ni, Pd, Pt) and $M(PH_3)_4(O_2)^+$, $M(PH_3)_4(C_2H_2)^+$, and $M(PH_3)_4(C_2H_4)^+$ (M = Co, Rh, Ir) by the HFS–Transition-State Method

TOM ZIEGLER

Received September 7, 1984

Hartree–Fock–Slater calculations are reported on the bonding energies for complexes between O_2, C_2H_2, or C_2H_4 and $M(PH_3)_2$ (M = Ni, Pd, Pt) or $M(PH_3)_4^+$ (M = Co, Rh, Ir). The calculated bonding energies follow within a triad the stability order 3d > 5d > 4d for a homologous series of complexes. The back-donation of charge from the metal center to the unsaturated ligands O_2, C_2H_2, and C_2H_4 was calculated to be more important for the stability of the complexes than the donation of charge from the ligands O_2, C_2H_2, and C_2H_4 to the metal center. The present study indicates that $M(PH_3)_2(O_2)$ and $M(PH_3)_4(O_2)^+$, in agreement with previous findings, can be formulated as superoxo complexes. The bond energies in an analogous series of complexes with O_2, C_2H_2, and C_2H_4 were calculated to follow the order $O_2 > C_2H_2 \sim C_2H_4$.

1. Introduction

Low-valent metal centers in d^8 ML_4 complexes as well as d^{10} ML_2 complexes are known[1] to form adducts with unsaturated XY molecules, such as O_2, alkenes, and alkynes, in which XY is bound side-on to the metal center.

The bonding between ML_n and XY was first accounted for by Dewar[2a] and by Chatt and Duncanson[2b] in terms of donation of charge from the occupied π orbital of XY to the metal center as well as back-donation of charge from the metal center to the unoccupied π^* orbital of XY. The understanding of the bonding in $ML_2(XY)$ and $ML_4(XY)$ complexes as well as in other $ML_n(XY)$ complexes has since the proposal of the Dewar–Chatt–Duncanson model been advanced considerably by a number of important theoretical investigation.[3]

We shall in the present study focus our attention on the strength of the bond between $M(PH_3)_2$ (M = Ni, Pd, Pt) and XY (XY = O_2, C_2H_2, C_2H_4) as well as the strength of the bond between $M(PH_3)_4^+$ (M = Co, Rh, Ir) and XY (XY = O_2, C_2H_2, C_2H_4). Such a systematic study should, together with the few available experimental data,[4] demonstrate the periodic trends along the two triads M = Ni, Pd, Pt and M = Co, Rh, Ir with respect to the bonding energy between ML_n and XY, as well as gauge the differences in the bonding modes of O_2, C_2H_2, and C_2H_4 to ML_n with respect to donation and back-donation.

All the calculations presented here have been based on the LCAO–HFS method by Baerends et al.[5] This method has previously been used in connection with studies on the bond between ethylene and various metal centers.[3f,g] The method has, in conjunction with the generalized transition-state method,[6] the distinct advantage of providing a breakdown of the calculated bonding energy between ML_n and XY in terms of steric factors as well as electronic contributions due to donation of charge from XY to ML_n and back-donation of charge from XY to ML_n.

The relativistic extension of the HFS method due to Snijders et al.[7] makes it possible in addition to analyze the contribution from relativistic effects to the bond between XY and the heavy 5d elements on ML_n.

2. Computational Details

All calculations have been based on the LCAO–HFS method due to Baerends et al.[5] and its relativistic extension due to Snijders et al.,[7] with a standard exchange factor of $\alpha = 0.7$. Bonding energies were calculated by the generalized transition-state method[6] both in the nonrelativistic case as well as the relativistic case. A triple ζ STO basis set[8] was used for 1s on H, 3p and 3s on P, 2s and 2p on C and O, and *n*s, *n*p, *n*d, $(n + 1)$s, and $(n + 1)$p on the metals (M), with two additional 3d orbitals added on P as polarization functions. The electrons in shells of lower energy on C, O, P, and M were considered as core electrons and treated by the frozen-core approximation according to the procedure due to Baerends et al.[5] The total molecular electron density was fitted in each SCF iteration by s, p, and d STO's centered on H, C, O, and P and s, p, d, F, and g STO's centered on the metal, in order to represent the Coulomb and exchange potentials accurately.

The following geometries have been used if not stated otherwise. The geometries of the model systems $M(PH_3)_4(O_2)^+$ (M = Co, Rh, Ir) were the same as those used by Norman and Ryan[3e,9] with the exception that the oxygen–oxygen distance was taken as 1.44 Å for all three complexes. The geometries of the model systems $M(PH_3)_2(O_2)$ (M = Ni, Pd, Pt) were taken from $M(PH_3)_4(O_2)^+$ (M = Co, Rh, and IR, respectively) by removing the two axial ligands in $M(PH_3)_4(O_2)^+$. The structure of $M(PH_3)_4(O_2)^+$ is shown in **6** and the structure of $M(PH_3)_2(O_2)$ in **5**.

For $M(PH_3)_2(C_2H_2)$ and $M(PH_3)_2(C_2H_4)$ (M = Ni, Pd, Pt), the $M(PH_3)_2$ fragments had the same geometry as in the corresponding $M(PH_3)_2(O_2)$ complex. The metal–carbon distances R_{MC} and the carbon–carbon distances R_{CC} in $M(PH_3)_2(C_2H_4)$ were as follows: Ni, 1.98 and 1.42; Pd, 2.12 and 1.43; Pt, 2.12 and 1.43, respectively, where the first entry refers to R_{MC} and the last entry to R_{CC} with both distances in Å. For $M(PH_3)_2(C_2H_2)$ the corresponding distances were taken as follows: Ni, 1.90 and 1.28; Pd, 2.04 and 1.29; Pt, (2.04 and 1.29, respectively. The HCC angle in C_2H_2 was taken as 145°, and the CC–CH_2

(1) (a) Hartley, F. R. *Angew. Chem.* **1972**, *84*, 657. (b) Vaska, L. *Acc. Chem. Res.* **1976**, *9*, 175.
(2) (a) Dewar, M. J. S. *Bull. Soc. Chim. Fr.* **1951**, *18*, C79. (b) Chatt, J.; Duncanson, L. A. *J. Chem. Soc.* **1953**, 2339.
(3) (a) Albright, T. A.; Hoffmann, R.; Thibeault, J. C.; Thorn, D. L. *J. Am. Chem. Soc.* **1979**, *101*, 3801. (b) Åkermark, B.; Almemark, M.; Almlof, J. Backwall, J.-E.; Roos, B.; Støgard, Å. *J. Am. Chem. Soc.* **1977**, *99*, 4617. (c) Sakaki, S.; Hori, K.; Ohyoshi, A. *Inorg. Chem.* **1978**, *17*, 3183. (d) Norman, J. G., Jr. *Inorg. Chem.* **1977**, *16*, 1328. (e) Norman, J. G., Jr.; Ryan, P. B. *Inorg. Chem.* **1982**, *21*, 3555. (f) Ziegler, T.; Rauk, A. *Inorg. Chem.* **1979**, *18*, 1558. (g) Baerends, E. J.; Oudshoorn, C.; Oskam, A. *J. Electron Spectrosc. Relat. Phenom.* **1975**, *6*, 259. (h) Hay, P. J. *J. Am. Chem. Soc.* **1984**, *106*, 5439. (i) Kitaura, K.; Sakaki, S.; Morokuma, K. *Inorg. Chem.* **1981**, *20*, 2292.
(4) (a) Mondal, J. U.; Blake, D. M. *Coord. Chem. Rev.* **1982**, *47*, 205. (b) Vaska, L.; Patel, R. C.; Brady, R. *Inorg. Chim. Acta* **1978**, *30*, 239. (c) Tolman, C. A.; Seidel, W. C.; Gosser, L. W. *Organometallics* **1983**, *2*, 1391. (d) Vaska, L. *Acc. Chem. Res.* **1968**, *1*, 335.
(5) (a) Baerends, E. J.; Ellis, D. E.; Ros, P. *Chem. Phys.* **1973**, *2*, 41. (b) Baerends, E. J.; Ros, P. *Int. J. Quantum Chem.* **1978**, *S12*, 169.
(6) Ziegler, T.; Rauk, A. *Theor. Chim. Acta* **1977**, *46*, 1.
(7) (a) Snijders, J. G.; Baerends, E. J. *Mol. Phys.* **1978**, *36*, 1789. (b) Snijders, J. G.; Baerends, E. J.; Ros, P. *Ibid.* **1979**, *38*, 1909. (c) Ziegler, T.; Snijders, J. G.; Baerends, E. J. *Chem. Phys.* **1981**, *74*, 1271.
(8) Snijders, G. J.; Baerends, E. J.; Vernooijs, P. *At. Data Nucl. Data Tables* **1982**, *26*, 483; and private communication. The triple-ζ basis for the $(n + 1)$p metal shell should have enough variational freedom to ensure that the conclusions drawn about the involvement from $(n + 1)$p in the bonding of the molecules under investigation are basis set independent. The STO exponents were as follows: Ni 0.95, 1.50, 2.50; Pd 0.80, 1.35, 2.35; Pt 1.10, 1.65, 2.65; Co 0.90, 1.40, 2.35; Rh 0.90, 1.50, 2.55; Ir 1.05, 1.65, 2.65.
(9) The following parameters have been taken from ref 3e. R_{MO} for M = Co, Rh, and Ir was 1.89, 2.04, and 2.04 Å, respectively. R_{MP_a} for M = Co, Rh, and Ir was 2.24, 2.39, and 2.39 Å, respectively. R_{MP_e} for M = Co, Rh, and Ir was 2.24, 2.32, and 2.32 Å, respectively. The angle P_aMP_a for M = Co, Rh, and Ir was 176, 161, and 161°, respectively. The angle P_eMP_e for M = Co, Rh, and Ir was 102, 94, and 95°, respectively. Here P_a and P_e refer to the axial P atom and the equatorial P atom in **4**.

0020-1669/85/1324-1547$01.50/0

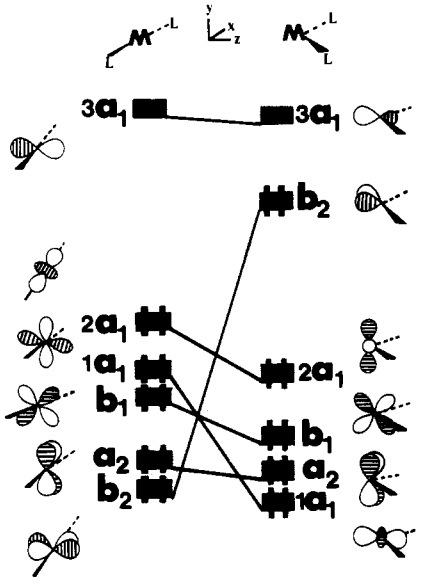

Figure 1. Orbital levels with schematic representation of the corresponding orbitals for d^{10} $M(PH_3)_2$ complexes in conformation **1** (left) as well as conformation **2** (right). The calculated orbital energies (eV) for $Pd(PH_3)_2$ in conformation **1** were as follows: b_2, −5.26; a_2, −5.20; b_1, −4.24; $1a_1$, −4.13; $2a_1$, −3.45; $3a_1$, −2.48. The energies (eV) for $Pd(PH_3)_2$ in conformation **2** were as follows: $1a_1$, −5.33; a_2, −5.21; b_1, −4.98; $2a_1$, −4.21; b_2, −2.90; $3a_1$, −0.98.

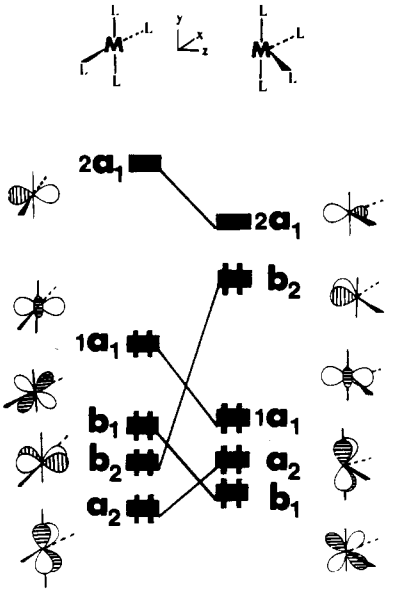

Figure 2. Orbital levels with schematic representation of the corresponding orbitals for d^8 $M(PH_3)_4^+$ complexes in conformation **3** (left) as well as conformation **4** (right). The energies (eV) for $Rh(PH_3)_4^+$ in conformation **3** were as follows: a_2, −9.21; b_2, −8.46; b_1, −8.31; $1a_1$, −7.28; $2a_1$, −4.93. The energies (eV) for $Rh(PH_3)_4^+$ in conformation **4** were as follows: b_1, −8.76; a_2, −8.69; $1a_1$, −8.03; b_2, −5.92; $2a_1$, −5.70.

dihedral angle in C_2H_4, as 28°. The C–H distances were 1.08 Å (C_2H_2) and 1.06 Å (C_2H_2), respectively, as in the free ligands. A HCH angle of 117° was used for C_2H_4. The geometries of $M(PH_3)_4(C_2H_2)^+$ and $M(PH_3)_4(C_2H_4)^+$ (M = Co, Rh, Ir) were derived from the corresponding 3d, 4d, and 5d complexes $M(PH_3)_2(C_2H_2)$ and $M(PH_3)_2(C_2H_4)$ by adding two axial PH_3 ligands.

3. Electronic Structure of $M(PH_3)_2$ (M = Ni, Pd, Pt) and $M(PH_3)_4^+$ (M = Co, Rh, Ir)

The d^{10} complexes ML_2 (M = Ni, Pd, Pt) are linear (**1**) in the free form and bent (**2**) when complexed to π ligands such as O_2, C_2H_2, and C_2H_4. The electronic structure of d^{10} ML_2 complexes

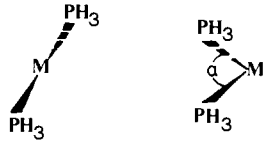

1 2

has been studied[10,11] extensively in conformation **1** as well as in conformation **2**. As a convenient starting point for the discussion in the following sections, we present a brief outline based on the diagram in Figure 1 where the upper valence levels of $M(PH_3)_2$ in the two conformations **1** and **2** are correlated. The highest occupied orbital (HOMO) $2a_1$ in **1** is antibonding with respect to the symmetrical σ ligand combination σ_s on the two PH_3 groups and the d_{x^2} metal orbital, $d_{x^2} = (3^{1/2}/2)d_{x^2-y^2} - (1/2)d_{z^2}$. The antibonding character of $2a_1$ is however reduced substantially by the involvement of $(n + 1)$s from the metal. The lowest unoccupied orbital of $M(PH_3)_2$ in **1** has a considerable contribution from $(n + 1)p_z$ on the metal. A reduction of the PMP angle α of $M(PH_3)_2$ from 180° makes it possible for d_{xz} on M to interact with the antisymmetrical σ combination σ_a from the two PH_3 ligands, and $b_2(d_{xz})$ evolves as the antibonding combination between d_{xz} and σ_a, which in **2** with 94° < α < 102° constitutes the HOMO of $M(PH_3)_2$ (see Figure 1) whereas $2a_1$, now less antibonding, has been lowered in energy. The LUMO in conformation **2** is an $(n + 1)$s, $(n + 1)p_z$ hybrid orbital. It should be noted that the antibonding character of b_2 in **2** is reduced by bonding interactions between σ_a and $(n + 1)p_x$ on the metal.

Steric factors would clearly favor conformation **1** over conformation **2**. Electronic factors treated on the level of the angular overlap method[11] with only d orbitals on the metal center would on the other hand not discriminate between **1** and **2** since the fully occupied d manifold (a_2, b_2, b_1, $1a_1$, and $2a_1$) is raised equally in energy in the two conformations. It can however be demonstrated from considerations based on second-order perturbation theory that electronic factors will favor **1** over **2** when $(n + 1)$s and $(n + 1)$p metal orbitals are included, since $(n + 1)$s can more effectively reduce the antibonding interaction between σ_s and d_{x^2} in **1** than $(n + 1)p_x$ can reduce the antibonding interaction between d_{xz} and σ_a in b_2 of **2**.

We have found from our HFS calculations on $M(PH_3)_2$ that **1** is favored over **2** by 34, 54, and 60 kJ mol^{-1} for M = Ni, Pd, and Pt, respectively. It is to be expected[12] on steric grounds that the energy difference between **1** and **2** will increase when PH_3 as a ligand is substituted with bulkier phosphines or phosphites, in particular for M = Ni with the shortest metal–P bond distance.

The d^8 complexes $M(PH_3)_4^+$ (M = Co, Rh, Ir) were assumed as the most stable conformation to have a pseudo-square-planar geometry **3** with a low-spin configuration.[13]

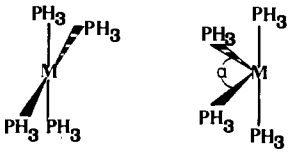

3 4

A correlation diagram between the upper orbital levels of $M(PH_3)_4^+$ in **3** and the upper orbital levels of $M(PH_3)_4^+$ in the butterfly geometry **4**, adopted in π complexes with O_2, C_2H_2, and C_2H_2, is given in Figure 2.

The HOMO $1a_1$ of $M(PH_3)_4^+$ in **3** is antibonding with respect to the ligand combinations and the d_{z^2} metal orbital. In conformation **4** with 94 ° < α < 102° the $b_2(d_{xz})$ orbital evolves as the HOMO whereas $1a_1(d_{z^2})$ has been lowered in energy as the

(10) Elian, M.; Hoffmann, R. *Inorg. Chem.* **1975**, *14*, 1058.
(11) Burdett, J. K. "Molecular Shapes"; Wiley Interscience: New York, 1980.
(12) Tolman, C. A. *Chem. Rev.* **1977**, *77*, 314.
(13) We are aware that $Co(PR_3)_4^+$ with bulky R groups adopts a tetrahedral geometry with a high-spin conformation in order to reduce the steric interaction between the PR_3 ligands.

antibonding interaction between the σ ligand combinations and the d_{z^2} metal orbital has been reduced. The LUMO of $M(PH_3)_4^+$ in **3** is primarily represented by $(n + 1)p_z$ whereas the LUMO of **4** is an $(n + 1)s$, $(n + 1)p_z$ hybrid. We note that[10] one member of the d manifold, $d_{x^2-y^2}$, is unoccupied in the three d^8 $M(PH_3)_4^+$ complexes. It has been raised in energy due to the antibonding interaction with the symmtrical σ combination of the PH_3 ligands. The $d_{x^2-y^2}$ orbital is slightly above the LUMO $2a_1$ in conformation **3** and more than 1 eV above the LUMO $2a_1$ in conformation **4**.

Steric factors would clearly favor **3** over **4** in $M(PH_3)_4^+$ just as they favored **1** over **2** in $M(PH_3)_2$. The electronic factors, which in $M(PH_3)_2$ only discriminated between **1** and **2** through the involvement of $(n + 1)s$ and $(n + 1)p$ orbitals on the metal, probably a small effect, will in $M(PH_3)_4^+$ favor **3** over **4** directly through the interactions between metal d orbitals and the σ ligand combinations, since the occupied part of the d manifold in **4** is destabilized more than in **3** by the antibonding interactions with the σ ligand combinations. This point can be shown readily by use of the angular overlap method.[11]

Our HFS calculations showed in line with the qualitative arguments given above that the differences in energy between **3** and **4** of $M(PH_3)_4^+$ in general are larger than the calculated differences in energy between **1** and **2** of $M(PH_3)_2$. We have calculated conformation **4** of $M(PH_3)_4^+$ to be 97, 160, and 166 kJ mol^{-1} higher in energy than conformation **3** of $M(PH_3)_4^+$ for M = Co, Rh, and Ir, respectively. The larger calculated differences in energy between **3** and **4** for M = Ir and Rh compared to those for M = Co is not surprising, since the σ overlaps between the d orbitals and the σ ligand combinations are larger for M = Ir and Rh than for M = Co. Thus, the relative destabilization of the occupied part of the d manifold in **4** compared to **3**, due to the antibonding interactions between d orbitals and the σ ligand combinations, will be more pronounced for the two elements Ir and Rh than for Co.

In the calculation of the energy differences between **1** and **2** as well as **3** and **4**, the angle α was changed without separate optimizations of the metal–phosphorus bond distances. A test calculation on $Pd(PH_3)_2$ showed that the difference in energy between **1** and **2** was increased from 54 to 59 kJ mol^{-1} when the Pd–P distances were optimized separately in **1** and **2**. We feel that a full optimization of the M–P distances will change the calculated energy differences between **1** and **2** as well as **3** and **4** slightly, without changing the trends discussed above.

4. Stability of $M(PH_3)_2(O_2)$ and $M(PH_3)_4(O_2)^+$

We shall now turn to a discussion of the bonding in the two dioxygen complexes $M(PH_3)_2(O_2)$ (**5**) and $M(PH_3)_4(O_2)^+$ (**6**).

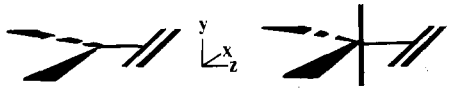

5 6

The bond energy ΔE_1 between $M(PH_3)_2$ and O_2 in $M(PH_3)_2(O_2)$, corresponding to the negative of the formation energy in the process

$$M(PH_3)_2 + O_2 = M(PH_3)_2(O_2) - \Delta E_1 \qquad (4.1)$$

is given by

$$\Delta E_1 = E[O_2] + E[M(PH_3)_2] - E[M(PH_3)_2(O_2)] \qquad (4.2)$$

where $E[M(PH_3)_2]$ is the energy of $M(PH_3)_2$ in conformation **1** and $E[M(PH_3)_2(O_2)]$ the energy of $M(PH_3)_2(O_2)$ in conformation **5**, whereas $E[O_2]$ corresponds to the energy of O_2 in the triplet ground state $^3\Sigma_g$ with the electron configuration $(1\sigma_g)^2(2\sigma_g)^2(1\sigma_u)^2(\pi_u)^4(\pi_{gx})(\pi_{gy})$ at the equilibrium distance R_{OO} = 1.21 Å.

The bonding energy ΔE_2 between $M(PH_3)_4^+$ and O_2 in **6**, corresponding to the negative of the formation energy for the process

$$M(PH_3)_4^+ + O_2 = M(PH_3)_4(O_2)^+ - \Delta E_2 \qquad (4.3)$$

is given by

$$\Delta E_2 = E[O_2] + E[M(PH_3)_4^+] - E[M(PH_3)_4(O_2)^+] \qquad (4.4)$$

where $E[M(PH_3)_4^+]$ is the energy of $M(PH_3)_4^+$ in conformation **3** with the low-spin configuration $(1a_1)^2(a_2)^2(b_1)^2(b_2)^2$ and $E[M(PH_3)_4(O_2)^+]$ the energy of **6**.

We shall now realize the two processes of eq 4.1 and 4.3 in a sequence of three steps. The choice of each step, if somewhat arbitrary, should hopefully help one to understand the bonding in **5** or **6**, and will in any case not influence the energies $-\Delta E_1$ and $-\Delta E_2$ for the overall processes in eq 4.1 and 4.3.

In the first step the three fragments $M(PH_3)_2$, $M(PH_3)_4^+$, and O_2 are given the geometries they will have in either **5** or **6**. Thus, $M(PH_3)_2$ and $M(PH_3)_4^+$ are given the geometries **2** and **4**, respectively, whereas R_{OO} in O_2 is changed from 1.21 to 1.44 Å. In the first step we retain the closed-shell low-spin electronic configurations of $M(PH_3)_2$ and $M(PH_3)_4^+$ but change the electronic structure of O_2 from $^3\Sigma_g$ to the configuration $(1\sigma_g)^2(2\sigma_g)^2(1\sigma_u)^2(\pi_u)^4(\pi_{gy})^2$ where one π^* orbital, π_{gx}, is fully vacated and one π^* orbital, π_{gy}, fully occupied. The change of geometry and electronic configuration in O_2 was calculated to require 258 kJ mol^{-1}. The energy contribution to the bonding energies ΔE_1 and ΔE_2 from the overall process in the first step is referred to as ΔE_{prep}.

In the second step the modified fragments are placed in the positions they will take up in either **5** or **6** while the electron pairs are confined to the orbitals they occupied in the separate modified fragments. Thus, occupied orbitals on one fragment are not yet allowed to interact with unoccupied orbitals on the other fragment. The energy contribution to the bonding energies ΔE_1 and ΔE_2 from the overall process in the second step, $\Delta E°$, is referred to as the steric interaction energy. It has an attractive (positive) contribution from the electrostatic interaction between the two fragments and a destabilizing (negative) contribution from the interactions between occupied orbitals on the two fragments, often referred to as repulsive four-electron interactions.

In the third step we allow the unoccupied and occupied fragment orbitals in each of the symmetry representations A_1, B_1, A_2, and B_2, corresponding to the C_{2v} point group symmetry of **5** and **6**, to interact. That is, we perform a complete nonrelativistic HFS calculation. The contribution from the third step to the bonding energies ΔE_1 and ΔE_2 is referred to as the electronic contribution ΔE_{elec}. We can further write ΔE_{elec} as $\Delta E_{elec} = \Delta E_{A_1} + \Delta E_{A_2} + \Delta E_{B_1} + \Delta E_{B_2}$, since[3f] ΔE_{elec} will have contributions from each symmetry representation. The total nonrelativistic bonding energy can now be written as $\Delta E_{prep} + \Delta E° + \Delta E_{A_1} + \Delta E_{A_2} + \Delta E_{B_1} + \Delta E_{B_2}$, by combining terms from the three steps.

We consider finally as a separate term the contribution from relativistic effects to the bonding energy, ΔE_R. We have found in a previous study,[7c] where ΔE_R is fully defined, that relativistic effects only contribute substantially to the bonding energy of transition-metal complexes when 5d elements are involved. The term ΔE_R is as a consequence only evaluated for M = Pt and Ir.

The calculated bonding energies, decomposed into the various contributions, are shown for the six dioxygen complexes in Table I. The contributions from ΔE_{prep} and $\Delta E°$ to the bonding energies are negative and destabilizing whereas the contribution from ΔE_{elec} is positive and stabilizing.

There are clearly two leading terms in ΔE_{elec}, namely ΔE_{A_1} and ΔE_{B_2}. The contribution from ΔE_{A_1} arises in $M(PH_3)_2(O_2)$ from the interaction between the LUMO $3a_1$ on $M(PH_3)_2$ and the occupied π orbital π_{ux} on O_2, as shown in **7a**, whereas ΔE_{A_1} in $M(PH_3)_4(O_2)^+$ is due to the interaction between the LUMO $2a_1$ on $M(PH_3)_4^+$ and the occupied π_{ux} orbital on O_2, as shown in **7b**.

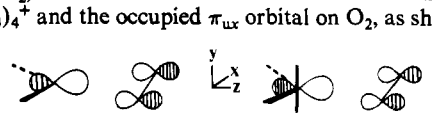

7a 7b

The interactions **7a** and **7b** represent in the Dewar–Chatt–Duncanson model[2] the donation of charge from O_2 to the metal center. The stability furnished by the donation is nearly the same

Table I. Decomposition of Calculated Bonding Energies (kJ mol^{-1}) for the Dioxygen Complexes

$ML_n(O_2)$	ΔE_{prep}	ΔE°	ΔE_{A_1}	ΔE_{A_2}	ΔE_{B_1}	ΔE_{B_2}	ΔE_R	ΔE^a
$Ni(PH_3)_2(O_2)$	−292.4	−334.8	112.7	1.8	24.2	734.7		246.2
$Pd(PH_3)_2(O_2)$	−311.8	−285.3	96.1	4.2	9.7	636.3		149.5
$Pt(PH_3)_2(O_2)$	−317.6	−288.8	95.9	0.4	13.1	634.7	31.2	168.9
$Co(PH_3)_4(O_2)^+$	−355.3	−372.9	133.6	11.6	40.9	724.5		182.4
$Rh(PH_3)_4(O_2)^+$	−418.3	−318.9	119.2	7.3	22.8	655.0		67.1
$Ir(PH_3)_4(O_2)^+$	−424.6	−327.2	127.4	6.6	21.3	647.3	29.1	79.5

[a] The total bonding energy ΔE is given by $\Delta E = \Delta E_{prep} + \Delta E^\circ + \Delta E_{A_1} + \Delta E_{A_2} + \Delta E_{B_1} + \Delta E_{B_2} + \Delta E_R$.

Table II. Decomposition of b_2, the Highest Occupied Orbital of $M(PH_3)_2$

$M(PH_3)_2$	$C_1(nd_{xz})^a$	$C_2(p_x)^a$	$C_3(\sigma_a)^a$	$\langle\pi_{gx}\|nd_{xz}\rangle^b$	$\langle\pi_{gx}\|(n+1)p_x\rangle^c$	$\langle\pi_{gx}\|b_2\rangle$
$Ni(PH_3)_2$	0.88	0.27	−0.43	0.1315	0.1474	0.1879
$Pd(PH_3)_2$	0.69	0.26	−0.72	0.1398	0.1153	0.1606
$Pt(PH_3)_2$	0.66	0.30	−0.77	0.1590	0.1164	0.1660

[a] The highest occupied orbital b_2 of $M(PH_3)_2$ can be written approximately as $b_2 = C_1[nd_{xz}] + C_2[(n+1)p_x] + C_3[\sigma_a]$, if we neglect contributions from other orbitals with coefficients numerically less than 0.20. [b] Overlap between nd_{xz} and π_{gx}. [c] Overlap between $(n+1)p_x$ and π_{gx}.

($\Delta E_{a_1} \sim 100$ kJ mol^{-1}) for all the dioxygen complexes; see Table I. A population analysis revealed that a charge of 0.3 e is donated to $3a_1$ or $2a_1$.

The term ΔE_{B_2}, corresponding to the interaction between the unoccupied π^* orbital, π_{gx}, on O_2 and either the HOMO b_2 on $M(PH_3)_2$ (**8a**) or the HOMO b_2 on $M(PH_3)_4^+$ (**8b**), represents

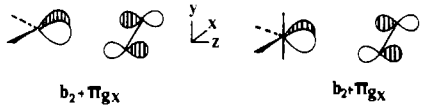

8a 8b

the back-donation of charge from the metal center to O_2 in the Dewar–Chatt–Duncanson model.[2] Nearly one full electron charge is back-donated to the π^* orbital of O_2 in each case, and the six systems can thus be characterized as superoxo complexes in agreement with previous findings.[3c,3e]

The stabilization of the dioxygen complexes from ΔE_{B_2} amounts to between 735 and 587 kJ mol^{-1} depending on the metal M, with the largest contribution for the two 3d elements Ni and Co. The back-donation of **8** is thus more important in terms of energy than the donation of **7** for the stability of $M(PH_3)_2(O_2)$ as well as $M(PH_3)_4(O_2)^+$.

The contribution from relativistic effects ΔE_R to the bonding energy was calculated to be small compared to both ΔE_{A_1} and ΔE_{B_2}, as shown in Table I. The influence of relativity is mainly that of reducing the four electron-destabilizing interactions in ΔE°, as discussed previously in ref 7c, whereas the change in the charge distribution induced by relativity was calculated to be small.

For metals of the same transition series the bonding energy in $M(PH_3)_2(O_2)$ was calculated to be about 80 kJ mol^{-1} larger than in $M(PH_3)_4(O_2)^+$; see Table I. The difference is primarily due to ΔE_{prep} and in our analysis can be traced back to a larger calculated difference in energy between **3** and **4** than between **1** and **2**, a point discussed in section 3. The 4d and 5d elements are calculated to form weaker dioxygen complexes than the 3d elements (Table I), with dioxygen complexes of the 5d elements being slightly more stable than the corresponding complexes of the 4d elements due[14] to ΔE_R.

It follows from Table I that ΔE_{B_2} is one of the terms responsible for the particularly strong bonds in $Ni(PH_3)_2(O_2)$ and $Co(PH_3)_4(O_2)^+$, since ΔE_{B_2} is calculated to be larger for Ni and Co than for the heavier congeners. In order to understand this point further, let us write an approximation of ΔE_{B_2} on the basis of perturbation theory:

$$\Delta E_{B_2} = k\frac{\langle\pi_{gx}|b_2\rangle^2}{\epsilon(\pi_{gx}) - \epsilon(b_2)} \qquad (4.5)$$

In eq 4.5 k is a positive constant[15] and $\langle\pi_{gx}|b_2\rangle$ is the overlap between the LUMO π_{gx} on O_2 with energy $\epsilon(\pi_{gx})$ and the HOMO b_2 on $M(PH_3)_2$ in conformation **2** of energy $\epsilon(b_2)$ or the HOMO b_2 of $M(PH_3)_4^+$ in conformation **4** with energy $\epsilon(b_2)$.

The denominator in eq 4.5 given by $\epsilon(\pi_{gx}) - \epsilon(b_2)$ is positive and represents the HOMO–LUMO gap for the interaction **8**. One might have expected the gap to be smallest in the case of the two 3d elements Ni and Co, since d-orbital energies are higher for atoms of Ni and Co than for atoms of Pd, Pt, Rh, and Ir as indicated to the left in **9**. A smaller gap $\epsilon(\pi_{gx}) - \epsilon(b_2)$ in the case

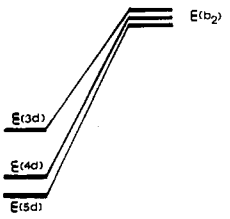

9

of the 3d elements would, according to eq 4.5, in turn have accounted nicely for the large ΔE_{B_2} term calculated for Ni and Co.

It is however important to note that b_2 is antibonding with respect to d_{xz} and the combination σ_a on the PH_3 ligands (see section 3) and that the antibonding interaction is strongest for the 4d and 5d elements with the largest σ overlap between d_{xz} and σ_a, as illustrated to the right in **9**. The orbital energy $\epsilon(b_2)$ of either $M(PH_3)_2$ or $M(PH_3)_4^+$ will as a consequence vary less alogn a triad than the energies of the d orbitals in the free atoms; see **9**. We have in fact calculated $\epsilon(b_2)$ for the three $M(PH_3)_2$ fragments to differ by less than 0.2 eV, and a similar small spread in energy was found for $M(PH_3)_4^+$ (M = Co, Rh, Ir). Variations in the HOMO–LUMO gap of **8a** or **8b** are as a consequence small and cannot be used to account for the large calculated ΔE_{B_2} term for Ni and Co.

The trend in ΔE_{B_2} can however be explained by considering the overlap integral $\langle\pi_{gx}|b_2\rangle$ in the numerator of eq 4.5. Our calculations indicate that $\langle\pi_{gx}|b_2\rangle$ is larger for M = Ni and Co than for M = Pd, Rh, Pt, and Ir. To understand this point, we refer to Table II, where b_2 is given for each of the three $M(PH_3)_2$ fragments, in terms of nd_{xz}, $(n+1)p_x$, and σ_a as $b_2 = C_1[nd_{xz}] + C_2[(n+1)p_x] + C_3[\sigma_a]$, along with the overlap integrals $\langle\pi_{gx}|nd_{xz}\rangle$, $\langle\pi_{gx}|(n+1)p_x\rangle$, and $\langle\pi_{gx}|b_2\rangle$. It follows from Table II that $\langle\pi_{gx}|b_2\rangle$ is larger for Ni than for Pd and Pt partly because

(14) Without the relativistic term ΔE_R the 4d elements would form slightly stronger dioxygen complexes than the 5d elements.

(15) The factor k is given by $\epsilon(b_2)^2$ in the angular overlap method and is thus constant along a triad in each of the two types of complexes $M(PH_3)_2(O_2)$ and $M(PH_3)_4(O_2)^+$, since $\epsilon(b_2)$ as discussed is nearly the same for 3d, 4d, and 5d elements.

Table III. Decomposition of Calculated Bonding Energies (kJ mol^{-1}) for the Ethylene Complexes

$ML_n(C_2H_4)$	ΔE_{prep}	ΔE°	ΔE_{A_1}	ΔE_{A_2}	ΔE_{B_1}	ΔE_{B_2}	ΔE_R	ΔE^a
$Ni(PH_3)_2(C_2H_4)$	−89.1	−149.9	94.2	0.3	17.3	294.1		166.9
$Pd(PH_3)_2(C_2H_4)$	−110.9	−145.9	72.2	1.3	18.1	263.4		98.2
$Pt(PH_3)_2(C_2H_4)$	−116.9	−179.1	87.9	2.1	21.5	265.8	23.3	104.6
$Co(PH_3)_4(C_2H_4)^+$	−152.2	−200.6	154.4	12.9	40.7	296.5		151.7
$Rh(PH_3)_4(C_2H_4)^+$	−217.3	−216.1	161.8	7.1	35.2	268.8		39.5
$Ir(PH_3)_4(C_2H_4)^+$	−222.9	−224.8	173.3	7.3	37.2	270.4	21.4	61.9

[a] The total bonding energy ΔE is given by $\Delta E = \Delta E_{prep} + \Delta E^\circ + \Delta E_{A_1} + \Delta E_{A_2} + \Delta E_{B_1} + \Delta E_{B_2} + \Delta E_R$.

Table IV. Decomposition of Calculated Bonding Energies (kJ mol^{-1}) for the Acetylene Complexes

$ML_n(C_2H_2)$	ΔE_{prep}	ΔE°	ΔE_{A_1}	ΔE_{A_2}	ΔE_{B_1}	ΔE_{B_2}	ΔE_R	ΔE^a
$Ni(PH_3)_2(C_2H_2)$	−115.1	−163.9	94.6	13.7	19.4	323.3		172.0
$Pd(PH_3)_2(C_2H_2)$	−137.4	−181.4	83.5	9.7	18.1	296.7		89.2
$Pt(PH_3)_2(C_2H_2)$	−143.4	−205.1	95.1	10.5	23.1	287.4	29.1	96.7
$Co(PH_3)_4(C_2H_2)^+$	−178.1	−216.0	165.4	12.1	39.1	317.4		139.9
$Rh(PH_3)_4(C_2H_2)^+$	−243.4	−228.3	170.4	9.4	29.7	282.7		20.5
$Ir(PH_3)_4(C_2H_2)^+$	−249.4	−236.3	177.8	9.7	28.6	294.9	32.1	57.5

[a] The total bonding energy ΔE is given by $\Delta E = \Delta E_{prep} + \Delta E^\circ + \Delta E_{A_1} + \Delta E_{A_2} + \Delta E_{B_1} + \Delta E_B + \Delta E_R$.

the strongly antibonding b_2 orbitals of $Pd(PH_3)_2$ and $Pt(PH_3)_2$ have a smaller participation from nd_{xz} than the modestly antibonding b_2 orbital of $Ni(PH_3)_2$ and partly because $(n+1)p_x$, although participating to the same extent in b_2 of the three $M(PH_3)_2$ fragments, has the largest overlap integral $\langle \pi_{gx}|(n+1)p_x\rangle$ in the case of Ni.

Only a few thermochemical data are available for the type of side-on dioxygen complexes studied here. The enthalpy of association for the addition of O_2 to *trans*-$[IrCl(CO)(PPh_3)_2]$ has been determined[4d] from kinetics data to be −71.5 kJ mol^{-1}. The enthalpy of association for the addition of O_2 to $Rh(cis\text{-}Ph_2PCH{=}CHPPh_2)_2^+$ was determined[4b] to be −46 kJ mol^{-1}. Qualitative observations based on equilibrium constants for O_2 association suggest,[4a] in agreement with the results of Table I, the stability order 3d > 5d > 4d within a triad.

5. Stability of $M(PH_3)_2(C_2H_2)$, $M(PH_3)_2(C_2H_4)$, $M(PH_3)_4(C_2H_2)^+$, and $M(PH_3)_4(C_2H_4)^+$

The decomposition scheme applied in section 4 to the dioxygen complexes can be used equally well to discuss the bonding in the ethylene complexes **10a** and the acetylene complexes **10b** with

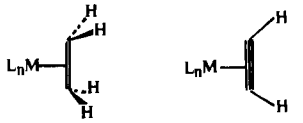

10a **10b**

either $M(PH_3)_2$ or $M(PH_3)_4^+$. Calculated bonding energies decomposed into the various components are given for ML_n–C_2H_4 in Table III and for ML_n–C_2H_2 in Table IV. The ethylene ligand, which in the free state is planar with R_{CC} = 1.34 Å, was given[3a,3i] a distorted geometry in **10a** with a CC–CH_2 dihedral angle of 28° and a C–C bond distance of 1.42–1.43 Å. The energy required for the distortion amounts to between 55 and 58 kJ mol^{-1}. The acetylene ligand, which in the free state is linear with R_{CC} = 1.20 Å, was given[3a,i] a bent structure in **10b** with CCH = 145° and a C–C bond distance of 1.28–1.29 Å. The deformation of C_2H_2 required between 81 and 84 kJ mol^{-1}.

The electronic structure of O_2 was changed from the ground-state configuration $(1\sigma_g)^2(2\sigma_g)^2(1\sigma_u)^2(\pi_u)^4(\pi_{gx})^1(\pi_{gy})^1$ to the excited configuration $(1\sigma_g)^2(2\sigma_g)^2(1\sigma_u)^2(\pi_u)^4(1\pi_{gy})^2$ in the first step toward the formation of ML_n–O_2, as discussed in section 4. Such a change in electronic conformation provided a fully unoccupied π^* orbital pointing toward the ML_n fragment in the spirit of the Dewar–Chatt–Duncanson model at a cost of 161 kJ mol^{-1}. A similar change in electronic configuration is of course not required for C_2H_2 and C_2H_4, since both ligands have a fully unoccupied π^* orbital. The contribution ΔE_{prep} to the bonding energy in either ML_n–C_2H_2 or ML_n–C_2H_4 is as a result numerically smaller than ΔE_{prep} for ML_n–O_2 (Tables I, III, and IV).

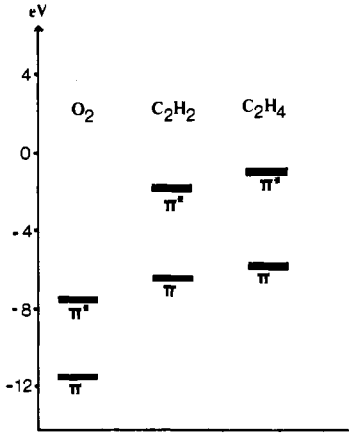

Figure 3. Energy diagram for the π and π^* orbitals of O_2, C_2H_4, and C_2H_2.

The bonding picture in either ML_n–C_2H_2 or ML_n–C_2H_4 is quite similar to that of ML_n–O_2. The π orbitals of C_2H_2 or C_2H_4 play much the same role in the donation process **7** as π_{ux} of O_2, whereas π^* of C_2H_2 or C_2H_4 has replaced π_{gx} of O_2 as the LUMO in the back-donation process **8**. The back-donation process is calculated in terms of energy (ΔE_{B_2}) to be more important for the stability of ML_n–C_2H_2 and ML_n–C_2H_4 than the donation process (ΔE_{A_1}) just as in the case of ML_n–O_2 (Tables I, III, and IV). We note further that ΔE_{B_2} is calculated to be much larger for ML_n–O_2 than for ML_n–C_2H_2 and ML_n–C_2H_4. This is not surprising in view of the fact that π^* of C_2H_2 and C_2H_4 is much higher in energy than π_{gx} of O_2, as shown in Figure 3. In terms of charge, 0.6 electron is transferred to π^* of C_2H_2 or C_2H_4 in the back-bonding process, as compared to a one-electron charge in the case of O_2.

The contribution from the donation process to the bonding energy (ΔE_{A_1}) is calculated to be larger for $M(PH_3)_4(C_2H_2)^+$ and $M(PH_3)_4(C_2H_4)^+$ than for $M(PH_3)_2(C_2H_2)$ and $M(PH_3)_2(C_2H_4)$. This trend can be accounted for by observing that $M(PH_3)_4^+$ is positively charged and that the LUMO ($2a_1$) is less than 0.5 eV above the HOMO (b_2) in $M(PH_3)_4^+$ (see Figure 2) whereas the separation between the LUMO ($3a_1$) and the HOMO (b_2) in the neutral fragments $M(PH_3)_2$ is 2 eV (Figure 1).

Ethylene and acetylene have qualitatively the same bonding mode, and we find in fact for a given ML_n fragment that the bonding energies are nearly the same in $ML_n(C_2H_2)$ and $ML_n(C_2H_4)$. The periodic trend in the bonding energies along a triad is further seen to follow the same stability order, 3d > 5d > 4d, as for the dioxygen complexes.

Kitaura et al.[3i] have carried out accurate ab initio calculations on $Ni(PH_3)_2(C_2H_2)$ and $Ni(PH_3)_2(C_2H_4)$, in which several key geometrical parameters were optimized. They too found, using

a decomposition scheme similar to that described in section 4, that the back-bonding in terms of energy (ΔE_{B_2}) is more important than the donation (ΔE_{A_1}) for the stability of $Ni(PH_3)_2(C_2H_2)$ and $Ni(PH_3)_2(C_2H_4)$. The calculated bonding energies were somewhat smaller than those obtained in the present work, 126 kJ mol^{-1} for $Ni(PH_3)_2(C_2H_4)$ and 154 kJ mol^{-1} for $Ni(PH_3)_2(C_2H_2)$.

Experimental bonding energies are not available for a homologous series of $ML_n(C_2H_2)$ or $ML_n(C_2H_4)$ complexes in which M is varied along a triad. It is however assumed, on the basis of experimental equilibrium constants for olefin and acetylene addition, that the stability order, in agreement with our findings, is 3d > 5d > 4d. For alkenes and alkynes complexed to $M(PR_3)_2$ bonding energies have only been determined for a few olefin complexes of $Ni(PR_3)_2$, via the reaction

$$Ni(PR_3)_4 + C_2H_4 = Ni(PR_3)_2(C_2H_4) + 2PR_3 \quad (5.1)$$

The determination of the bonding energy from eq 5.1 is however somewhat hampered by the lack of accurate values for the energy required to dissociate two PR_3 ligands from $Ni(PR_3)_4$. Tolman et al.[4c] give in their latest estimate a bonding energy of 167 kJ mol^{-1} for $Ni(P(O\text{-}p\text{-tolyl})_3)_2(C_2H_4)$. The good agreement between this value and a calculated bonding energy of 166.9 kJ mol^{-1} for $Ni(PH_3)_2(C_2H_4)$ (Table III) is clearly fortuitous. One wouuld in fact expect the bonding energy of $Ni(PH_3)_2(C_2H_4)$ to be larger than the bonding energy of $Ni(P(O\text{-}p\text{-tolyl})_3)_2(C_2H_4)$, since the deformation of $Ni(PR_3)_2$ from **1** to **2** on steric grounds must require more energy for R = O-*p*-tolyl than for R = H. The bonding energy for alkenes and alkynes complexed to $M(PR_3)_4^+$ can be determined directly via the process

$$M(PR_3)_4^+ + XY = M(PR_3)_4(XY)^+ \quad (5.2)$$

For $Ir(PPh_3)_2(CO)Cl$ the bonding energies with C_2H_4 and C_2H_2 were determined[4a] in solution to be 49.4 and 38.9 kJ mol^{-1}, respectively. Data from analogous complexes of Co and Rh are not available.

We have calculated the $M(PH_3)_2$ fragments to form stronger π complexes with C_2H_2 and C_2H_4 than the $M(PH_3)_4^+$ fragments in spite of the larger contribution from ΔE_{A_1} to the stability of $M(PH_3)_4(C_2H_2)^+$ and $M(PH_3)_4(C_2H_4)^+$. The difference in stability can, just as for the dioxygen complexes, be traced to ΔE_{prep} and the substantial energy required to deform $M(PH_3)_4^+$ from conformation **3** to conformation **4**. It should however be pointed out that d^{10} complexes of Ni, Pd, and Pt with phosphine ligands exist as $M(PR_3)_4$ or $M(PR_3)_3$ species rather than in the coordinatively unsaturated form $M(PR_3)_2$. The formation of the d^{10} complex $M(PR_3)_2XY$ will as a consequence require the dissociation of one or two PR_3 ligands (see eq 5.1), and $M(PR_3)_2(XY)$ might for this reason not be more readily formed than $M(PR_3)_4(XY)^+$.

6. Concluding Remarks

Our approach is approximae, aside from the inherent limitations of the HFS method, since we have been forced of necessity to represent the ML_2 and ML_4 fragments by $M(PH_3)_2$ or $M(PH_3)_4^+$ model systems using standard structural parameters rather than optimized geometries. It has however been possible within such limitations to carry out a systematic study of unsaturated ligands such as O_2, C_2H_2, and C_2H_4, complexed to d^{10} ML_2 fragments as well as d^8 ML_4 fragments.

Our calculations indicate that d^{10} ML_2 fragments as well as d^8 ML_4 fragments of 3d elements form stronger π complexes with the unsaturated ligands O_2, C_2H_2, and C_2H_4 than the corresponding ML_n fragments of the 4d and 5d elements, and we have given in section 4 a possible rationale for this trend.

We have further found, on the basis of an energy decomposition analysis, that the back-donation in the Dewar–Chatt–Duncanson model in terms of energy is more important for the stability of the systems discussed here than the donation. It has also been demonstrated that the ML_4 fragments are less prone to form π complexes than the ML_2 fragments, as a substantial energy is required to deform the pseudo-square-planar conformation **3** of ML_4 in the free state to the butterfly geometry **4** adopted in the $ML_4(XY)$ complexes.

Our calculations indicate finally that the bonding energies in an analogous set of complexes with O_2, C_2H_2, and C_2H_4 follow the order $O_2 > C_2H_2 \sim C_2H_4$.

Acknowledgment. This investigation was supported by the Natural Sciences and Engineering Research Council of Canada (NSERC).

Contribution from the Department of Chemistry,
Monash University, Clayton, Victoria 3168, Australia

Magnetic Properties and Zero-Field Splitting in High-Spin Manganese(III) Complexes. 1. Mononuclear and Polynuclear Schiff-Base Chelates

BRENDAN J. KENNEDY and KEITH S. MURRAY*

Received June 11, 1984

Variable-temperature (4.2–300 K) and variable-field (4.2 K, 5–50 kG) susceptibility measurements have been made on a range of manganese(III) Schiff-base complexes. The compounds studied contain either tetradentate salicylaldimines and β-ketone imines of the types [Mn(salen)X] and [Mn(acen)X], where X is Cl^-, Br^-, OAc^-, SCN^-, N_3^-, or bidentate salicylaldimines of the type $Mn(sal\text{-}NR)_3$. The measurements were generally made on Vaseline mulls of the samples in order to avoid anomalous results due to crystallite alignment. Spin Hamiltonian theory has been used to deduce values of the zero-field splitting parameter, D, and the exchange coupling parameter, J. The D values fall in the range −1 to −4 cm^{-1}. J values of less than −1 cm^{-1} were detected in some of the "monomers" and up to −5.4 cm^{-1} in the dimer or linear-chain examples. In linear chains such as [Mn(salen)OAc] and [Mn(salen)N_3] a small interchain exchange contribution was required to completely explain the data.

Introduction

High-spin manganese(III) complexes have a ^5D ground term that is split in octahedral crystal fields to produce $^5T_{2g}$ and ^5E_g terms. The effect of noncubic symmetry and/or Jahn–Teller distortions is to remove the oribtal degeneracy of the ^5E_g ground term to give an orbital singlet lowest, either a $^5A_{1g}$ or $^5B_{1g}$ (in D_{4h} symmetry). The spin degeneracy of the ground state is further removed by spin–orbit coupling, giving rise to the so-called

0020-1669/85/1324-1552$01.50/0